THE ISO VIEW OF STAR FORMING GALAXIES

G. Helou
California Institute of Technology, Pasadena, California, USA

ABSTRACT

ISO studies of normal galaxies in the local Universe have revealed new basic properties with significant implications for the star formation process and cosmology. This paper will review the general results of a statistical nature, provide a glimpse of the profusion of results on individual objects, and explore some of the resulting insights.

Key words: normal galaxies; star formation; interstellar medium.

1. INTRODUCTION

The Infrared Space Observatory (ISO, Kessler et al. 1996) took infrared astronomy in space to new levels of sensitivity and a new realm of spectroscopy across the whole spectrum from 3 to 200μm. Its versatile instrumentation took to the rich and fascinating extragalactic infrared sky first revealed by IRAS, and moved our knowledge of that sky an order of magnitude further and deeper. The unfettered access to the spectrum in space and low thermal backgrounds gave ISO a tremendous advantage in studying galaxies regardless of redshift, and allowed it to tackle much lower surface brightness sources. The spectroscopic capabilities of all four instruments were especially valuable tools in characterizing the interstellar gas, dust and radiation field, and at constraining the overall energetics and star formation rate. It was thus able to extend the KAO studies of starburst nuclei to the less intense star formation in normal galaxies.

This article will review significant ISO contributions to understanding normal galaxies, defined as those systems whose energetics are dominated by nucleosynthesis with negligible contributions by an active galactic nucleus. Normal galaxies account for most of the star formation in the Universe, and therefore for the bulk of its chemical evolution. ISO data on normal galaxies should thus bridge the gap between the details of nearby systems and the cosmic history of star formation, one of the more prominent questions in cosmology today. Because of their diversity, understanding galaxies requires studying them as an ensemble, and in particular as a sequence with increasing levels of star formation activity, up to and including the most extreme. While this review will attempt to present the whole activity sequence, ultraluminous galaxies and nuclear starbursts are more extensively covered in Alan Moorwood's review (these proceedings).

2. THE MID-INFRARED SPECTRAL ENERGY DISTRIBUTION

In the integrated spectra of galaxies, the mid-infrared marks the transition from star-dominated emission to interstellar dust reradiation providing the luminosity. ISO has shown the details of this transition for the first time by providing continuous coverage, and filling in some crucial details as discussed in this and the next two sections. The relevant data were acquired with ISOPHOT, PHT-S module from 2.5 to 5 and from 5.7 to 11.6$\,\mu$m (Lemke et al. 1996); with ISOCAM in the CVF (Circular Variable Filter) mode from 5 to 16.5 (Cesarsky et al. 1996); and with SWS from 2.5 to 45$\,\mu$m (de Graauw et al. 1996).

The transition from stellar to interstellar emission is well illustrated by the spectra of Virgo Cluster galaxies collected by Boselli et al. (1998). Its precise location and therefore the interpretation to attach to mid-infrared fluxes can be parametrized by the ratio of far-infrared, say as measured by IRAS, to visible light fluxes. Interstellar dust emission takes over by 5$\,\mu$m when this ratio exceeds 0.5, and at shorter wavelengths for higher ratios. As might be expected, Elliptical galaxies are dominated by stellar emission, both photospheric and from circumstellar dust shells, and therefore provide the templates that one subtracts to isolate the interstellar emission component in Spiral galaxies (Boselli, Lequeux & Contursi 1997; Madden, Vigroux & Sauvage 1997). In addition, ISO sensitivity has allowed us to study the small amounts of interstellar medium (ISM) contained in Elliptical galaxies, and to look into differences with the ISM of Spirals (Knapp et al. 1996; Fich et al. , Madden et al. & Malhotra et al. in these proceedings; note also the study of E+A galaxies in the Coma Cluster by Quillen et al. in preparation).

2.1. The aromatic features

IRAS data had already indicated (Beichman 1987; Puget & Léger 1989) that the mid-infrared emission from the ISM was dominated by small fluctuating grains and Aromatic Features in Emission (AFE). ISO has not only established into fact what had been hypothesis (Figure 1), but is also allowing us to address quantitatively the mid-infrared energy budget across various emission components, and to investigate the variation of this budget among various galaxies.

The AFE appear in two main groups, one stretching from 5.5 to $9\,\mu$m, with peaks at 6.3, 7.7 and 8.6, and the other one starting at $11\,\mu$m and extending to $12.5\,\mu$m (Lu et al. these proceedings; Helou et al. 1999). There is good evidence linking these features to Polycyclic Aromatic Hydrocarbons (PAH), but no rigorous spectral identification of specific molecules (Tielens these proceedings; Puget & Léger 1989; Allamandola et al. 1989). It is generally agreed that the emitters are small structures, no more than a few hundred atoms, transiently excited to high energy levels by single photons. The AFE together carry 5 to 20% of the "FIR" luminosity between 40 and $120\,\mu$m as defined in Helou et al. (1988), this percentage being generally smaller in more active galaxies (Lu et al. in these proceedings). Boselli et al. (1997 and 1998) have interpreted similar trends as evidence for the destruction of AFE carriers in more intense radiation fields (see also Helou, Ryter & Soifer 1991).

In addition to the AFE, there is a clear though weak continuum detection at $\lambda < 5\,\mu$m, and an apparently unrelated continuum component at $\lambda > 13\,\mu$m, which becomes dominant in active systems as discussed in section 3 below. The relation of the continua in these two spectral ranges is still unclear, making it hard to derive by interpolation a description of the continuum in $5 < \lambda < 13\,\mu$m where the Aromatic Features dominate.

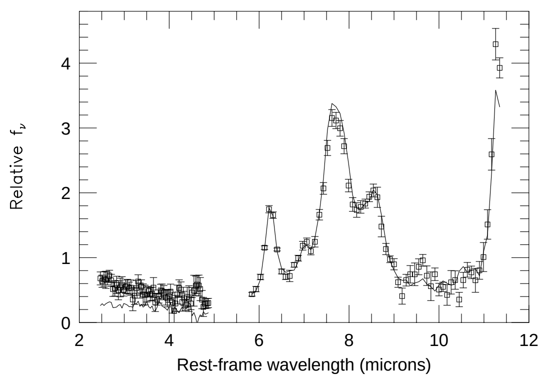

Figure 1. Two composite mid-infrared spectra, one for twelve FIR-cold galaxies (squares), and one for twelve FIR-warm ones (connected dots). Spectra were averaged after normalization to the 6.3 μm peak.

The relative fluxes in individual Aromatic Features depend very weakly on galaxy parameters such as the far-infrared colors, as illustrated in Figure 1. This is direct evidence that the emitting particles are not in thermal equilibrium. The strongest detectable effect in Figure 1 is the slightly stronger $11.3\,\mu$m feature in the colder galaxies. Since this feature is linked primarily to neutral PAHs as opposed to the shorter wavelength features which have a strong ionized PAH contribution (Tielens, these proceedings), one is tempted to interpret this trend as a result of the more active galaxies having a greater contribution to their luminosity originating in regions heated by harder radiation fields. The continuum at $\lambda < 5\,\mu$m is still subject to calibration uncertainties, but might amount to as much as three percent of the total infrared luminosity in some systems. It has a slope close to zero in f_ν *vs.* ν (connected dots in Figure 1), whose extrapolation to longer wavelengths would place it below the observed flux density even at $9-10\,\mu$m. It is almost certainly of non-stellar origin, and is probably due to fluctuating grains without aromatic features.

Rouan et al. (1996), Block et al. (1997) and Smith (1998) have combined ISOCAM and Brγ images with other broad-band and line images to estimate star formation rates, ISM parameters, obscuration and dust properties. These studies again point to Aromatic Feature carriers as a ubiquitous component of interstellar dust, to the likely destruction of these carriers by ionizing UV, and to dust heating in non-starburst disk galaxies being derived from both old stars and OB stars.

ISOCAM CVF studies between 5 and $17\,\mu$m are turning out to be powerful diagnostics of the radiation field in the disks of nearby galaxies, allowing us to disentangle the variations in heating intensity and hardness of interstellar radiation. The approach is to relate the intensity to the shape of the continuum, and the hardness to the ratios of ionic fine-structure lines (Tran 1998; Contursi 1998). See also, in these proceedings, the overview on ISOCAM studies of nearby galaxies by Vigroux et al., the studies of NGC 891 by Le Coupanec et al. and by Mattila et al., and of low-metallicity dwarf galaxies by Madden et al. (in preparation).

2.2. High-redshift applications

Since the spectral signature in Figure 1 applies to the majority of star-forming galaxies, it can be used as a template to obtain redshifts of highly extincted galaxies with the next infrared observatory, NASA's SIRTF (Space InfraRed Telescope Facility). For instance, a galaxy at a redshift z=3 with a flux density average of 0.5 mJy in the range $19-27\,\mu$m and a total infrared luminosity comparable to Mkn 231 at $\sim 3\times10^{12}\,L_\odot$ would be detected by the SIRTF IRS (Infrared Spectrometer; Roellig et al. 1998) in roughly 1000 seconds of integration (D.W. Weedman, private communication).

In surveys with fixed spectral bands, the Aromatic Features will result in a unique K-correction as redshift takes them in and out of the bands. The detection probability would be enhanced or lessened for certain redshift intervals, causing ripples in source counts as a function of flux; Xu et al. (1998) have modelled this effect for NASA's WIRE (Wide-Field InfraRed Explorer; Hacking et al. 1999) mission. However, this effect has already been manifested with ISO, in deep 15 μm imaging data in the direction of galaxy clusters. These observations were aimed at detecting background objects boosted by gravitational lensing, thus allowing the survey to penetrate further in space and time. In the Barvainis et al. (1999) survey, one out of every five galaxies detected in the direction of each of Abell 2218 and Abell 2319 turns out to be at a redshift near 1, the others being at redshifts of 0.3 or less. A redshift of 1 places the main clump of Aromatic Features squarely in the 15 μm band, enhancing the probability of detection. Similar results from a more extensive survey are reported by Metcalfe et al. (these proceedings), and by Fadda et al. (these proceedings).

As the early Universe opens up for mid-infrared exploration, the properties of low metallicity star-forming galaxies become more relevant as a template for high-redshift galaxies. ISO has provided the data for constructing such templates, both from studies of low metallicity dwarf galaxies (Madden et al., and Sauvage & Thuan in these proceedings), and the study of nearby galaxy disks with significant metallicity gradients such as M 101 (Vigroux et al. these proceedings).

2.3. Exceptions

The "standard" spectra described above characterize the integrated emission from normal galaxies, but exceptions arise at extreme conditions, and are easiest to detect in specific ISM phases of individual galaxies. At the smallest scales in the most intense parts of HII regions, Contursi (1998) and Tran (1998) report spectra which depart significantly from the standard ones in the location and strength of features. Similarly distorted spectra are also observed in NGC 4418 (Lu et al. 1999), and close to the Active Nucleus of Cen A (Vigroux et al. , these proceedings). This radical transformation in the spectrum must then result from extremely UV-rich heating radiation, and most likely reflects severe modification of the emitting grains, including the destruction of Aromatic Feature carriers. Significant distortions in the spectrum driven by a rising continuum but without radical changes in the Aromatic Features have also been reported by Lutz et al. (1998) in extremely active galaxies. The mid-infrared spectra of starbursts are relatively "standard", whereas galaxies with an active Black Hole nucleus have a continuum rising towards longer wavelengths with insignificant Aromatic Features. Ultra-Luminous Infrared Galaxies show intermediate spectra, modified in addition by large optical depths (Genzel et al. 1998).

At the other end of the heating sequence, Cesarsky et al. (1998) report that the 5–9 μm Aromatic Features are missing from the emission of the bulge and of the quiet parts of the bright infrared ring in M 31. The 11.3 and 12.7 μm features are present, perhaps a result of their originating primarily on neutral PAHs. The relatively weak and UV-poor heating radiation in these parts of M 31 cannot alone explain the absence of Aromatic Features, for other studies (e.g. Uchida et al. 1998) show that photons of a few eV are sufficient to generate the standard spectrum. It would appear that the dust properties are again modified, this time by prolonged shielding from UV processing in the astration cycle. Additional evidence of abnormal ISM properties in the same regions are found by Lequeux et al. (1999) in their study of the broad-band mid-infrared emission.

Another peculiar exception is provided by Sauvage & Thuan (these proceedings) in SBS 0335-052, a blue compact dwarf with a metallicity about 1/40 solar. None of the Aromatic Features are detected here, and the spectrum appears best fit by highly extincted blackbody emission. The authors propose the early chemical age of the system as the most likely reason behind the absence of the Aromatic Features, though one cannot rule out the possibility that the UV radiation from the intense star formation episode also plays a role in the destruction of the Aromatic Feature carriers. If this spectrum does indeed characterize all low metallicity objects, one would expect the "standard" spectrum to disappear gradually as a function of increasing redshift, thus making it harder to detect the Aromatic signature of dust and distinguish star formation from Black Hole activity as the energy source in the earliest systems.

3. THE 7-TO-15 μm COLORS

A large number of extragalactic broad-band measurements was collected by ISOCAM (Cesarsky et al. 1996) at wavelengths between 4 and 18μm, previously inaccessible with such sensitivity and versatility. Two photometric bands were most widely used for observations of nearby as well as distant and more luminous galaxies, namely the "LW2" band centered at 6.75 μm, and the "LW3" band centered at 15 μm. The LW2 filter was designed to capture mostly AFE emission, whereas LW3 was aimed at the continuum range beyond the bulk of the AFE, though it ends up with a small contribution from the last feature at 12.5 μm. The CVF mode of ISOCAM between 5 and 17 μm has also proven quite powerful in its ability to image both line and continuum emission. The overview by Vigroux et al. in these proceedings summarizes what has been learnt to date from these data, including the interpretation of the mid-infrared images and their relation to star formation rates.

The ISOCAM images of galaxies show dust emission in nuclear regions, in the inner barred disk, outlining the spiral arms, and tracing the disk out to the Holmberg radius and beyond (Malhotra et al. 1996, Sauvage et al. 1996, Vigroux 1997, Smith 1998, Roussel et al. in these proceedings). There are clear color variations within spiral galaxies, some of which have not yet found satisfactory explanations (Helou et al. 1996; Tran 1998).

The 6.75-to-15 μm color ratio formed from ISOCAM bands however has emerged as an interesting diagnostic of the radiation environment. This ratio remains relatively constant and near unity as the ISM of galaxies proceeds from quiescent to mildly active. As dust heating increases further, the 15 μm flux increases steeply compared to 6.75 μm, pointing to a significant contribution by dust at color temperature

100 K < T_{MIR} < 200 K, typical of a heating intensity up to 10^4 times that of the diffuse interstellar radiation field in the local Milky Way (Helou et al. 1997). While such a temperature could result from classical dust heated within or just outside HII regions, there is no decisive evidence as to the size of grains involved. It is simpler at this time to associate this component empirically with the observed emission spectrum of HII regions and their immediate surroundings (Tran 1998; Contursi 1998). This emission has severely depressed AFE, and is dominated by a steeply rising though not quite a blackbody continuum, consistent with mild fluctuations in grain temperatures, $\Delta T/T \sim 0.5$. This HII region hot dust component becomes detectable in systems where the color temperature from the 60-to-100 μm ratio is half T_{MIR}, demonstrating the broad distribution of dust temperatures within any galaxy. The combined data from ISO and IRAS on these systems are consistent with an extension of the "two-component model" of infrared emission, which describes galaxies as a linear combination of a quiescent medium and a star-forming medium, and where the mixing ratio determines the colors of each system (Helou 1986). This color behavior was observed in the sample of galaxies used for the Key Project on normal galaxies conducted under NASA Guaranteed Time (Helou et al. 1996), and confirmed in the sample of galaxies observed under ISOCAM Guaranteed Time (see figure in Vigroux et al. in these proceedings).

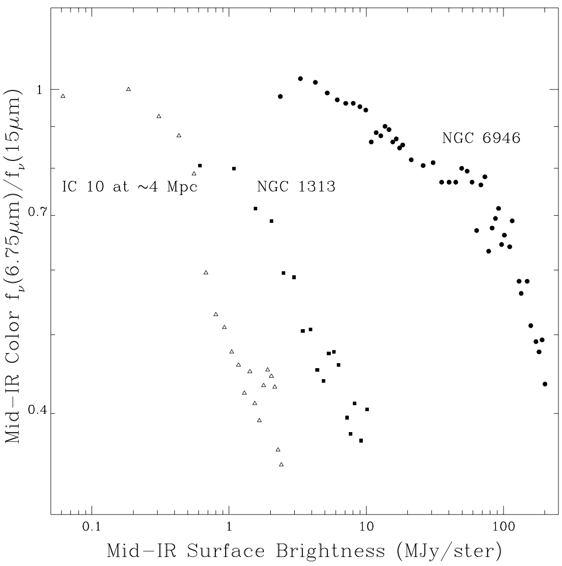

Figure 2. The mid-infrared color as a function of surface brightness for three disk galaxies well resolved by ISOCAM, and smoothed so the resolution corresponds to $\lesssim$200 pc in each case (Dale et al. 1999). All three data sets show roughly the same behavior, indicative primarily of how color and surface brightness evolve as heating intensity increases. The data are consistent with the expectation that a change in total ISM column density will shift the curves along the surface brightness axis: NGC 6946 does indeed have a total HI about an order of magnitude greater than the other two galaxies.

Similar behavior is observed within the disks of star forming galaxies, where the 6.75-to-15 μm color drops precipitously as the surface brightness exceeds a certain threshold (Dale et al. 1999). The point of inflexion in the color curve occurs at a variable surface brightness which is a function of the dust column density, whereas the shape of the curve seems invariant, and may result from a rise in both the hardness and intensity of the heating radiation (Figure 2). Dale et al. (1999) conclude that the mid-infrared surface brightness rise is driven primarily by column density while colors are determined mostly by heating intensity.

4. THE GLOBAL INFRARED SPECTRUM

Turning now to the long wavelength end of the spectrum, photometry at $120 - 200\,\mu$m using ISOPHOT is starting to constrain the distribution of dust temperatures at low heating levels, especially in nearby well resolved galaxies such as M31 (Haas et al. 1998, and in these proceedings), M51 or M101 (Hippelein et al. 1996), where cold dust dominates the luminosity. Similar analysis on more active galaxies is also under way (e.g., Klaas et al. 1997; Klaas, Haas & Schulz in these proceedings) to obtain the best possible estimates of the total infrared emission and therefore of the dust mass. Alton et al. (1998) have reported that the 200 μm emission is more extended than at shorter wavelengths in several galaxies. This result however hinges closely on a very precise knowledge of the beam shapes at various wavelengths, which was not yet achieved as of this writing.

A proper determination of the total infrared luminosity and the long-wavelength spectral shape in normal galaxies is critical to estimating the contribution of galaxies to the infrared and submm extragalactic background light, and thereby deriving the infrared term in the star formation history of the Universe. While work on the ISOPHOT calibration continues, one could estimate an improved infrared spectral energy distribution by combining the mid-infrared results described above with existing IRAS data. Such a rough estimation is presented in Table 1 for three different levels of activity in galaxies, parametrized by the 60-to-100 μm ratio. It should be noted that all information in Table 1 at $\lambda > 100\,\mu$m is based on modelling IRAS data using a power-law distribution of dust mass as a function of heating intensity. Table 1 illustrates the general trend, but also ignores variations in spectral shape at constant 60-to-100 μm ratio, including intrinsic scatter in the ratio of mid-infrared to far-infrared (Lu et al. in these proceedings). The 20 to 40 μm range appears to show the most significant growth in relative terms as the activity level increases, at the expense of the submillimeter. Even after ISO, our knowledge of the detailed shape of the spectrum in this range remains limited, and may not improve significantly until the launch of SIRTF.

5. MOLECULAR SPECTRAL LINES

One of the great achievements of ISO was the detection of the long-sought molecular hydrogen tran-

Table 1. Rough energy distribution across the infrared spectrum for galaxies with various levels of star formation activity, parametrized by the IRAS color in the first column. Each column heading gives the wavelength range over which the spectrum is integrated, and the table entries are the fractions of total infrared luminosity appearing in that range. The spectral range in column 6 corresponds to the "FIR" synthetic band (Helou et al. 1988).

$\frac{f_\nu(60\,\mu m)}{f_\nu(100\,\mu m)}$	F(3–5μm)	F(5–13μm)	F(13–20μm)	F(20–42μm)	F(42–122μm)	F(122–1100μm)
0.40	$\lesssim$0.02	0.12	0.04	0.10	0.40	0.29
0.72	$\lesssim$0.01	0.07	0.04	0.17	0.52	0.18
0.94	$\lesssim$0.01	0.04	0.04	0.22	0.56	0.13

sitions from rotationally excited states, and the realization of their promise as accurate tracers of the H_2 mass (e.g., Draine & Bertoldi in these proceedings), allowing for the first time a direct gauge of the dominant phase of the ISM. Most of the H_2 data were collected by the SWS (de Graauw et al. 1996). Several of these lines, especially S(0), S(1) and S(2) were detected in galaxies early in the ISO mission, permitting a detailed discussion of the gas phase conditions and heating mechanisms. Valentijn et al. (1996) for instance studied the nuclear star burst of NGC 6946. Because of their high excitation levels however, these lines tend to trace H_2 warmer than $\sim$ 100 K, and are therefore easier to detect in the more intense star formation environments (Kunze et al. 1996; Kunze et al. in these proceedings). Still, Valentijn & van der Werf (these proceedings) report the detection of H_2 emission from the extended disk of the edge-on galaxy NGC 891. They detect S(0) and S(1) at eight positions, tracing the emission out to 12 kpc from the nucleus of the galaxy, and derive H_2 temperature constraints and molecular mass estimates.

Hydroxyl (OH) was also detected in starburst galaxies, but in absorption rather than emission. A first report by Skinner et al. (1997) showed OH absorption at 35 μm in the spectrum of Arp 220, and confirmed for the first time pumping by infrared photons as the excitation mechanism behind OH megamasers. Bradford et al. (these proceedings) report OH in absorption at 35, 53 and 119μm in NGC 253, and resolve the line at 119μm with the LWS Fabry-Pérot mode. They estimate total column and excitation temperatures for the OH, and constrain the geometry of the molecular material and its relationship to the infrared-emitting dust. A similar study of NGC 4945 by Lord et al. (in preparation) finds consistency between the properties derived from OH data and [CII] 157.7 μm and [OI] 63.2 μm data. Lord et al. also report water vapor lines in absorption in the same object.

6. FAR-INFRARED FINE-STRUCTURE LINES

Far-infrared fine structure lines, [CII] 157.7 μm and [OI] 63.2 μm in particular, have long been used for estimating density and radiation intensity in photodissociation regions (PDR) (e.g., Hollenbach & Tielens 1997). ISO-LWS (Clegg et al. 1996) has provided for this topic a wealth of data, whose interpretation is creating controversy and challenging theoretical models. Malhotra et al. (1997) showed that while two thirds of normal galaxies have $\mathcal{L}(\mathrm{CII})/\mathcal{L}(\mathrm{FIR})$ in the range $2-7\times10^{-3}$, this ratio decreases on average as the 60-to-100 μm or the $\mathcal{L}(\mathrm{FIR})/\mathcal{L}(\mathrm{B})$ ratios increase, both indicating more active star formation (Figure 3). They linked this decrease to elevated heating intensities, which ionize grains and thereby reduce the photo-electric yield.

The same CII deficiency is also observed in ultraluminous infrared galaxies (Luhman et al. 1998), where optical depth effects have been proposed as the origin of the effect. This is hard to reconcile however with a similar deficiency effect observed for [NII] 121.9 μm, but not for [OI] 63.2 μm. Fischer et al., Luhman et al. and Malhotra et al. (these proceedings) give updated discussions of this topic, while Lord et al. and Unger et al. (in preparation) discuss PDR properties in NGC 4945 and Cen A.

Stacey et al. (these proceedings) present detailed maps of M 83 in several fine-structure lines, and point to the importance of low density HII regions as a source of [CII] emission. This same contribution by diffuse PDRs is invoked by Pierini et al. (these proceedings) in explaining the low [CII]-to-CO ratios in quiescent Virgo cluster galaxies. Using the same Virgo galaxies data, Leech et al. (in preparation) report a trend of decreasing [CII]/FIR ratios as galaxies become less active in star formation. Combining the results of Leech et al. with those of Malhotra et al. work leads to a picture where [CII]/FIR rises by an order of magnitude as galaxies move away from complete quiescence, reaches a broad maximum for normal galaxies actively forming stars, then decreases again by more than an order of magnitude as galaxies begin to approach the extreme properties of starbursts.

What could be behind this behavior? At the quiescent end, the relative lack of ionizing photons in the stellar spectrum could naturally explain the low values of [CII]/FIR. UV-poor heating would on one hand lower CII abundance, and on the other hand yield less energetic photo-electrons, so a less energetic CII excitation would be expected. At the starburst end, the extreme excitation conditions could generate lower photo-electric efficiency as proposed by Malhotra et al. (these proceedings). There is evidence however pointing in a different direction, namely that the relative drop in [CII] is due to a decrease in the concentration of the grains crucial for the photo-electric effect. It is well known (e.g. Hollenbach & Tielens 1997) that the smallest grains such as the carriers of AFE are responsible for the bulk of photo-electric yield in a PDR. Depletion of these carriers would weaken the coupling between radiation

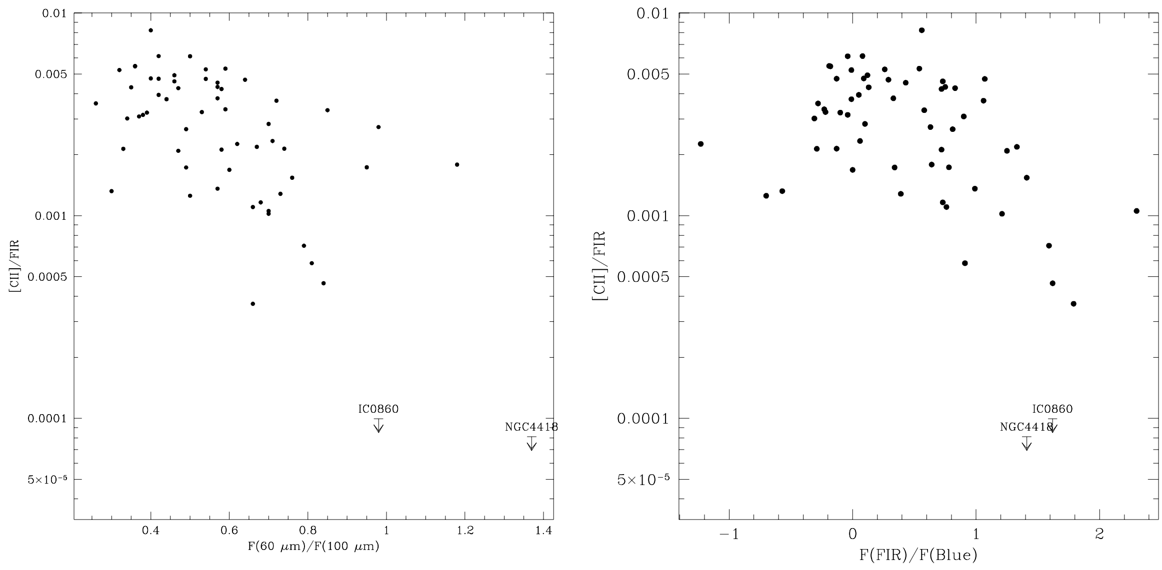

Figure 3. The CII deficiency in active star forming galaxies from Malhotra et al. (1997). See also Malhotra et al. (these proceedings).

field and gas, and lead to weaker fine-structure line emission compared to total dust re-radiation. The evidence in question is that unlike [CII]/FIR, the ratio of [CII] to AFE flux does not decrease in normal galaxies with increasing activity (Helou et al. 1999). This suggests that the emissions from [CII] and AFE originate in the same regions of the ISM, so their ratio is dictated by the physics of the photo-electric effect and remains constant, whereas [OI] and FIR originate from distinctly warmer and denser regions, so that the changing ratio [CII]/FIR, just like [CII]/[OI], reflects the systematic shift in density distribution of the ISM as galaxies approach star-burst conditions.

7. MORE STUDIES

In addition to the topics covered above, the ISO archive will soon offer a wealth of data on a wide variety of extragalactic subjects affecting our understanding of normal galaxies. Studies in galaxy clusters and groups for instance have targeted the population of medium-distant clusters at z=0.1–0.3 (Lémonon et al. , Fadda & Elbaz in these proceedings), or the location of enhanced infrared emission in compact groups (Latorre et al. in preparation). Stickel et al. (1998) have reported the detection of intracluster dust in Coma at 200μm, and related it to the cooling flows revealed by X-ray observations, while Xu, Sulentic & Tuffs (1999) have studied intergalactic star formation in Stefan's Quintet using mid-infrared data. Charmandaris et al. and Gallais et al. (these proceedings) have taken a detailed look at some of the nearest interacting galaxy systems in order to study collisionally induced star formation.

Beichman et al. (in preparation) and Gilmore & Unavane (in preparation) report on deep searches for mid-infrared haloes around edge-on galaxies, and place upper limits on the contribution to the missing mass by low-mass stars. Jarrett et al. (these proceedings) report on mid-infrared detection of a bridge of interstellar gas and magnetized plasma created between two galaxies after a collision which caused the two disks to pass through each other and entangle the interstellar media.

Observations of Local Group members allow detailed analysis of the ISM and star formation on the few pc scale, and are a crucial stepping stone to understanding the integrated emission in more distant objects. In these proceedings, such detailed studies of HII and star formation regions regions, or of the stellar population in the Magellanic Clouds are reported by Comeron & Claes, Henning et al. , Loup et al. , Missoulis et al. , and Vermeij & van der Hulst.

8. CONCLUSIONS

ISO studies of normal galaxies have already yielded major progress in our grasp of their phenomenology, especially in the areas of mid-infrared spectra and images, global spectral energy distribution, and far-infrared fine-structure lines. The improved phenomenology is reshaping our physical understanding of galaxies, in particular in terms of

1. better decomposition of the infrared luminosity into a distribution of dust mass as a function of heating intensity, based on the infrared spectrum and images;

2. more precise constraints on the density and intensity in the active ISM based on fine-structure lines, surface brightness, and the spectral decomposition above;

3. more accurate estimates of the molecular gas content based on H_2 data and other molecular lines.

The improved characterization and insights move us closer to formulating a dynamical model for star formation on the scale of galaxies, which would be a major step towards deriving the cosmological history of star formation in the Universe. In addition, they are key to understanding the extremely high luminosity objects, which are the beacons we must use in exploring the early Universe.

This progress leads to more informed planning for upcoming surveys or missions. SIRTF, SOFIA, FIRST and PLANCK will build on ISO, and eventually address the new puzzles that ISO will leave behind.

ACKNOWLEDGMENTS

I would like to thank all those colleagues who generously provided data and graphics for this review. Danny Dale and Nanyao Lu helped by providing customized plots and helpful discussions. I would like to acknowledge the patience of the editors, and their assistance with the manuscript, and Mary Ellen Barba for her negotiating skills. This work was carried out at the California Institute of Technology, under contract with the National Aeronautics and Space Administration, as part of the ISO Data Analysis Funding Program.

REFERENCES

Allamandola, L. J, Tielens, A. G. G. M., & Barker, J. R. 1989, ApJS, 71, 733

Alton, P.B. et al. 1998, A&A, 335, 807

Barvainis, R., Antonucci, A. & Helou, G. 1999, ApJ, submitted

Beichman, C.A. 1987, ARA&A, 25, 521

Block, D.L., Elmegreen, B.G., Stockton, A. & Sauvage, M. 1997, ApJL, 486, L95

Boselli, A., Lequeux, J. & Contursi, A. 1997, A&A, 324, L13

Boselli, A. et al. 1998, A&A, 335, 53

Cesarsky, C. et al. 1996, A&A, 315, L32

Cesarsky, D., et al. 1998, A&A, 337, L35

Clegg, P. et al. 1996, A&A, 315, L38

Contursi, A. 1998, *PhD Thesis*, Univ. de Paris

Dale, D. et al. 1999, in preparation

de Graauw, T. et al. 1996, A&A, 315, L49

Genzel, R. et al. 1998, ApJ, 498, 579

Haas, M., Lemke, D., Stickel, M. et al. 1998, A&A, 338, L33

Hacking, P. et al. 1999, *Astrophysics with Infrared Surveys: A Prelude to SIRTF*, PASP Conf Series, in press

Helou, G. 1986, ApJL, 311, L33

Helou, G. et al. 1988 ApJS, 68, 151

Helou, G., Ryter, C. & Soifer, B.T. 1991, ApJ, 376, 505

Helou, G. et al. 1996 A&A, 315, L157

Helou, G., Becklin, E., Stencel, R.E. & Wilkes, B. 1997, *ASP Conf Ser* 124, 393

Helou, G., Lu, N., Werner, M.W., Malhotra, S. & Silbermann, N. 1999, ApJ, submitted

Helou et al. 1999, in preparation

Hippelein, H. et al. 1996, A&A, 315, L79

Hollenbach, D.J. & Tielens, A.G.G.M. 1997, ARA&A, 35, 179

Kessler, M.F. et al. 1996, A&A, 315, L27

Klaas, U., Haas, M., Heinrichsen, I. & Schulz, B. 1997, A&A, 325, L21

Knapp, G.R., Rupen, M.P., Fich, M., Harper, D.A. & Wynn-Williams, C.G. 1996, A&A, 315, L75

Kunze, D. et al. 1996, A&A, 315, L101

Lemke, D. et al. 1996, A&A, 315, L64

Lequeux, J. et al. , A&A, submitted

Lu, N. et al. 1999, in preparation

Luhman, M.L. et al. 1998, ApJL, 504, L11

Lutz, D., Spoon, H.W.W., Rigopoulou, D., Moorwood, A.F.M. & Genzel, R., 1998, ApJ, 505, L103

Madden, S.C., Vigroux, L. & Sauvage, M. 1997, in *Extragalactic Astronomy in the Infrared*, ed. Mamon, Thuan & Van (Editions Frontières: Paris)

Malhotra, S. et al. 1996, A&A, 315, L161

Malhotra, S. et al. 1997, ApJ, 491, L27

Metcalfe, L. et al. 1996, A&A, 315, L105

Puget, J.-L. & Léger, A. 1989, ARA&A, 27, 161

Roellig, T.L., Houck, J.R., Van Cleve, J. et al. 1998, SPIE, in press

Rouan, D. et al. 1996, A&A, 315, L141

Sauvage, M. et al. 1996, A&A, 315, L89

Skinner, C.J., Smith, H.A., Sturm, E., Barlow, M.J., Cohen, R.J. & Stacey, G.J. 1997, Nature, 386, 472

Smith, B. 1998, ApJ, 500, 181

Smith, B.J. & Madden, S. C. 1997, AJ, 114, 138

Stickel, M. et al. 1998, A&A, 336, 116

Tran, D. 1998, *PhD Thesis*, Univ. de Paris

Uchida, K., Sellgren, K. & Werner, M., 1998, ApJ, 493, L109

Valentijn, E.A. et al. 1996, A&A, 315, L60

Vigroux, L. 1997, in *Extragalactic Astronomy in the Infrared*, ed. G. Mamon, T.X. Thuan & J.T.T. Van (Editions Frontières: Paris)

Xu, C. et al. 1998, ApJ, 508, 576

Xu, C., Sulentic, J.W. & Tuffs, R. 1999, in preparation